

# SENSITIVITIES IN LARGE EDDY SIMULATION AND IMPROVED ESTIMATES OF TURBULENT FLOW FUNCTIONALS \*

MIHAI ANITESCU<sup>†</sup> AND WILLIAM J. LAYTON<sup>‡</sup>

**Abstract.** We consider a prototypical problem: simulate velocity and pressure in a turbulent flow using large eddy simulation (LES) and then use the results to estimate the force the underlying turbulent flow exerts on an immersed body. For eddy viscosity-type LES models we develop the appropriate continuous sensitivity equation and show how it can improve the functional estimate by using the sensitivity with respect to the user-selected length scale to incorporate the effects of the underlying unresolved small-scale fluctuations on the functionals sought.

**Key words.** Large eddy simulations, sensitivity, turbulence.

**AMS subject classifications.** 76D05, 35Q30, 90C31.

**1. Introduction.** For the foreseeable future, computational resources will be insufficient for the direct numerical solution of most turbulent flow problems. On the other hand, important decisions are made and significant designs produced based on estimates of quantities in turbulent flow that are simulated by using various models of turbulence. Even when using the model that current practice considers best for a particular application, often the reliability of the model's predictions for the specific application is not assessed. This situation is particularly troublesome because solutions of turbulence models can display sensitivity with respect to the user-elected model parameters, in addition to the sensitivity with respect to the upstream flow, subgrid model, and numerical realization of it (reported by Sagaut and Lê [19]).

For example, calculating the force a fluid exerts on an immersed body, such as lift or drag, involves first solving the Navier-Stokes equations

$$(1.1) \quad \begin{aligned} u_t + \nabla \cdot (u u) + \nabla \cdot \sigma(u, p) &= f, \text{ in } \Omega \times (0, T) \\ \sigma(u, p) &:= pI - 2\nu \nabla^s u, \quad \nabla^s u := \frac{1}{2}(\nabla u + \nabla u^t), \\ \nabla \cdot u &= 0, \text{ in } \Omega \times (0, T), \quad u = 0 \text{ on } \partial\Omega \text{ and } u(x, 0) = u_0(x), \text{ in } \Omega. \end{aligned}$$

If  $B$  denotes the boundary of the immersed body, next the force must be calculated on  $B$ :

$$(1.2) \quad \begin{aligned} \text{force on } B &= \int_B \hat{n} \cdot \sigma ds = \int_B \hat{n} \cdot [pI - 2\nu \nabla^s u] ds, \\ \hat{n} &= \text{outward unit normal to } B. \end{aligned}$$

This calculation requires accurate estimation of  $p$  and derivatives of  $u$  on the flow boundary—a problem harder than accurately predicting the turbulent velocity itself.

The basic approach used for turbulent flows has been to replace the Navier–Stokes equations (1.1) by a turbulence model and then insert the velocity-pressure predicted

---

\*This paper is developed from a 2003 research note with a similar title.

<sup>†</sup>Argonne National Laboratory, Mathematics and Computer Science Division, Argonne, IL 60439  
anitescu@math.pitt.edu

<sup>‡</sup>University of Pittsburgh, Department of Mathematics, Pittsburgh, PA 15260,  
wj1@pitt.edu, <http://www.math.pitt.edu/~wj1>

by the turbulence model into the right-hand side of the functional, such as (1.2). Uncertainties arise immediately, however, because of the typical sensitivity to the model's input parameters. Perhaps more important, turbulence models approximate flow averages. Thus, all the information on fluctuations is lost in them. However, the small-scale fluctuations can have a determining role in functionals such as (1.2). Mathematically, the reason that the derivatives occurring in (1.2) overweigh velocity changes occurring across small distances. One concrete example is drag in the flow over a dimpled vs. smooth golf ball; a related example is riblets. Both change the geometry (and flow) on scales below typical feasible meshes. Indeed, drag reduction strategies of injection of small amounts of microbubbles or polymers near a body are, in part, based on the expectation that a little power input to alter the flow's small scales can have a large effect on the global drag.

This paper considers functional estimation and solution sensitivity for models arising in large eddy simulation. In Section 2 we apply the continuous sensitivity idea to a common class of large eddy simulation models. The sensitivity equation approach has the great advantage of giving computable quantitative estimates of the local sensitivity of the model's predicted flow field to variations in the input parameters. Thus, a sensitivity calculation will show in which regions the predicted velocities are reliable and hence believable and in which regions those predicted velocities are highly sensitive and hence should be viewed with greater suspicion. We focus on the case of sensitivity with respect to the user-selected length scale  $\delta$ . The reason for this focus is (Section 3) that the sensitivity of the flow with respect to variations in  $\delta$  can be used to improve the estimate of flow functionals, such as lift and drag, which can depend strongly on the unknown and unresolved turbulent fluctuations.

**2. The Sensitivity Equation of Eddy Viscosity Models.** The continuous sensitivity equation approach is becoming increasingly important in computational fluid dynamics but is not yet a common tool in large eddy simulation of turbulence. In this section we apply the sensitivity idea to find the continuous sensitivity equation with respect to variations in the cutoff length scale  $\delta$ . For a general treatment of sensitivities and applications to other flow problems, see (among many interesting works) [3, 4, 10, 9, 20].

Suppose a local spatial filter has been selected (denoted by an overbar) associated with the length scale  $\delta$ . Filtering the Navier-Stokes equations leads to the problem of closure, and one common class of closure models is based on the Boussinesq, or eddy viscosity, hypothesis. The model we consider takes the general form of finding the approximate large-scale velocity  $w(x, t)$  approximately  $w$  and pressure  $q(x, t)$  satisfying  $\nabla \cdot w = 0$  and

$$(2.1) \quad w_t + \nabla \cdot (w \otimes w) - \nu \Delta w + \nabla q - \nabla \cdot (\nu_T(\delta, w) \nabla^s w) = \bar{f},$$

where  $\nu$  is the kinematic viscosity,  $\bar{f}$  is the space filtered body force, and  $\nu_T$  is the eddy viscosity coefficient that must be specified to select the model. As an example, the Smagorinsky model, while not considered the best, is perhaps the most commonly used model and is given by the eddy viscosity choice

$$(2.2) \quad \nu_T = \nu_{\text{Smag}}(\delta, w) := (C_s \delta)^2 |\nabla^s w|, \quad C_s \sim 0.1.$$

For other eddy viscosity models see the presentation in [18, 13, 2, 16, 12]. Once the Smagorinsky constant,  $C_s$ , and the initial and boundary conditions are specified, for

a given  $\delta$  the equations (2.1), (2.2) uniquely determine a solution  $w, q$  implicitly as a function of  $\delta$ <sup>1</sup>.

DEFINITION 2.1. *Let  $w, q$  be the solution of (2.1). The sensitivity of  $w, q$  to variations in  $\delta$  is defined to be the derivatives of  $w, q$  with respect to  $\delta$ ,*

$$w_\delta := \frac{\partial w}{\partial \delta}, \quad q_\delta := \frac{\partial q}{\partial \delta}.$$

One can easily derive continuous equations for the sensitivities by implicit differentiation of (2.1), with respect to  $\delta$ . Doing so gives the equations  $\nabla \cdot w_\delta = 0$  and

$$(2.3) \quad w_{\delta,t} + \nabla \cdot (w w_\delta + w_\delta w) - \nu \Delta w_\delta + \nabla q_\delta - \nabla \cdot \left( \left[ \frac{\partial}{\partial \delta} \nu_T(\delta, w) + \frac{\partial}{\partial w} \nu_T(\delta, w) \cdot w_\delta \right] \nabla^s w + \nu_T(\delta, w) \nabla^s w_\delta \right) = \frac{\partial}{\partial \delta}(\bar{f})$$

Thus, once the large eddy velocity and pressure,  $w, q$ , are calculated, the corresponding sensitivities can be found by solving a linear problem for  $w_\delta, q_\delta$  that is precisely the nonlinear large eddy simulation model linearized about  $(w, q)$ . Thus, sensitivities can be quickly and economically calculated by modifying the program used to calculate  $(w, q)$ . On the other hand, one can simply use an unmodified program to test whether sensitivity information will be useful for a given application before beginning program modifications. This approach involves solving the model for  $w(\delta_1)$  and  $w(\delta_2)$  for  $|\delta_1 - \delta_2|$  small and computing sensitivities by means of the divided difference

$$s = \frac{w(\delta_2) - w(\delta_1)}{\delta_2 - \delta_1}.$$

In our numerical simulating in Section 5 we use the latter approach.

For the Smagorinsky model we have  $\nu_T = (C_s \delta)^2 |\nabla^s w|$ . Thus the bracketed term is

$$(2.4) \quad [\nu_{T,\delta} + \nu_{T,w} \cdot w_\delta] = 2C_s \delta |\nabla^s w| + (C_s \delta)^2 \left( \frac{\nabla^s w}{|\nabla^s w|} \right) : \nabla^s w_\delta.$$

**2.1. Calculating  $\bar{f}_\delta = \frac{\partial}{\partial \delta} \bar{f}$ .** If the body forces acting on the flow are smooth enough,  $\bar{f}_\delta$  is negligible. Otherwise, the right-hand side of (2.3)  $\bar{f}_\delta$  can play an important role in the sensitivity equation because it incorporates information about body force fluctuations. When  $f$  is not smooth, the exact value of  $\bar{f}_\delta$  depends on the precise filter specified. When  $\bar{f}$  is defined by convolutions, extending  $f$  by zero off the flow domain and then defining

$$\bar{f} := \int_{\mathbf{R}^d} \delta^{-d} g\left(\frac{x'}{\delta}\right) f(x - x') dx, \quad g(x) := \text{chosen filter kernel},$$

then  $\bar{f}_\delta$  can be calculated explicitly.

When  $\bar{f}$  is defined by using differential filters [7, 16, 13, 2], a small modification is needed that depends on the exact differential filter specified. Two interesting differential filters are defined by solving the shifted Poisson problem for  $\bar{f}$ ,

$$(2.5) \quad -\delta^2 \Delta \bar{f} + \bar{f} = f, \text{ in } \Omega, \quad \bar{f} = 0 \text{ on } \partial\Omega,$$

---

<sup>1</sup>Fundamental theoretical questions arise even at this first step. For example, it is not known whether the solution of the Smagorinsky model is a  $C^1$  function of  $\delta$  for  $\delta > 0$  or whether the branch is continuous down to  $\delta = 0$ .

and by solving the shifted Stokes problem for  $\bar{f}$ ,

$$(2.6) \quad -\delta^2 \Delta \bar{f} + \bar{f} + \nabla \lambda = f \text{ and } \nabla \cdot \bar{f} = 0, \text{ in } \Omega, \text{ and } \bar{f} = 0 \text{ on } \partial\Omega.$$

The second differential filter (2.6) preserves incompressibility and is thus interesting in spite of its costing more than the first.

With the first filter  $\bar{f} = (-\delta^2 \Delta + 1)^{-1} f$ , we differentiate implicitly with respect to  $\delta$  to derive an equation for  $\bar{f}_\delta$ :

$$(-\delta^2 \Delta + 1) \bar{f}_\delta = 2\delta \Delta \bar{f} = (\text{via (2.4)}) = \left(-\frac{2}{\delta}\right)(f - \bar{f}).$$

Thus,

$$(2.7) \quad \bar{f}_\delta = \left(-\frac{2}{\delta}\right) (\bar{f}').$$

Analogously, we obtain the initial condition for  $w_\delta$

$$(2.8) \quad w_\delta(x, 0) = \bar{u}_{0,\delta}(x) = \left(-\frac{2}{\delta}\right) (\bar{u}'_0).$$

Here, we denote by  $h'$  the fluctuation of a function  $h(x)$ , that is,  $h' = h - \bar{h}$ .

**2.2. Boundary Conditions for the Sensitivities.** Boundary conditions for sensitivities must be specified. The most interesting and important cases are sensitivity with respect to the (modeled) upstream conditions and the (modeled) outflow conditions [19]. At this point, a mathematical formulation of the former is unclear, whereas there exist many options for the latter. Thus we consider here only boundary conditions for the sensitivities at solid walls.

With a differential filter like (2.5) and (2.6) the boundary conditions for the sensitivities are clear because there exist no error and no variability with respect to  $\delta$  in the conditions for  $w$  on the wall:  $w_\delta = 0$  on the boundary.

Some slight modifications of the wall models are necessary to compute sensitivities when near-wall models are used. These are usually associated with averaging; see [6] for some mathematical issues involved. Many near-wall models or numerical boundary conditions are possible. For specificity and clarity we treat the simplest ones considered in, for example, [14], in which the large structure's action on the boundary are modeled by no penetration and slip with friction conditions:

$$w \cdot \hat{n} = 0 \text{ and } \beta(\delta, \nu) w \cdot \hat{\tau}_j + \hat{n} \cdot (\nu \nabla^s w) \cdot \hat{\tau}_j = 0, \text{ on } \partial\Omega,$$

where  $\hat{n}$  is the unit normal to the boundary and  $\hat{\tau}_1, \hat{\tau}_2$  are a system of tangent vectors on the boundary. Implicit differentiation with respect to  $\delta$  gives the boundary conditions for the sensitivities:

$$w_\delta \cdot \hat{n} = 0 \text{ and } \beta(\delta, \nu) w_\delta \cdot \hat{\tau}_j + \hat{n} \cdot (2\nu \nabla^s w_\delta) \cdot \hat{\tau}_j = -\beta_\delta(\delta, \nu) w \cdot \hat{\tau}_j \text{ on } \partial\Omega.$$

Since  $\beta(\delta)$  increases monotonically to infinity as  $\delta \rightarrow 0$ , [14],  $\beta_\delta > 0$ . Thus, slippage in the flow velocity  $w$  acts to decrease the slippage in the sensitivities when they are aligned and increase it when they are opposed.

**3. Improving Estimates of Functionals of Turbulent Quantities.** The usual procedure to estimate a flow functional is to compute the LES velocity  $w$  approximating the fluid motion on scales larger than the cut-off length scale and then to approximate the sought solution functional  $J(u)$  by  $J(w)$ . This can be a reasonable approximation when the small scales do not influence the functional and when  $w$  is a good approximation to the large scales of  $u$ . When the functionals involve derivatives of  $u$ , however, those derivatives tend to overweigh the small scales in the functional. We show in this section how the approximation of  $J(u)$  can be improved to incorporate some of the unresolved scale effects through sensitivity information. Numerical tests of the improvement of flow functionals by using sensitivity information (with accompanying mathematical support) have yielded positive results for a different eddy viscosity model in [17].

We suppose that the LES solution  $w$  implicitly defines a smooth function of  $\delta$ ,  $w = w(\delta)$ , with the property that

$$(3.1) \quad w(\delta) \rightarrow u \text{ as } \delta \rightarrow 0.$$

This is a minimal analytic consistency condition for a large eddy simulation, which nevertheless has so far been proven to hold for only a few large eddy models; see, for example, [5, 15]. If the functional is  $C^1$ , then the composition

$$\delta \mapsto J(w(\delta)) =: J(\delta)$$

defines a smooth map. The value  $J(\delta) = J(w(\delta))$  is computable while  $J(u) = J(w(0)) = J(0)$  is sought. Since  $\delta$  is small, the linear approximation to  $J(0)$  is justified. This yields the following approximation to  $J(u)$ :

$$(3.2) \quad J(u) \doteq J(w(\delta)) - \delta J'(w(\delta)) \cdot w_\delta.$$

The increment  $\delta J'(w(\delta))$  incorporates effects of unresolved scales on  $J(u)$  and is computable once the solution sensitivities  $w_\delta$  are calculated.

If the functional itself is regularized,  $J(u)$  is approximated by a  $\delta$  dependent approximation  $J(\delta, w(\delta))$ . Then (3.2) is modified by

$$(3.3) \quad J(u) \doteq J(\delta, w(\delta)) - \delta(J_w(\delta, w(\delta)) \cdot w_\delta + J_\delta(\delta, w)).$$

**3.1. Example: Lift, Drag, and Other Fluid-Boundary Interactions in Turbulent Flows.** In many applications, forces exerted by fluid on boundaries must be estimated. In this case the functional is given by

$$(3.4) \quad J(u, p) := \oint_B \hat{n} \cdot [pI - 2\nu \nabla^s u] \cdot \hat{a} \, ds,$$

where  $\hat{a}$  is a unit vector and  $B$  is the boundary of the immersed body. If  $\hat{a}$  points in the direction of motion,  $J(u)$  represents drag, whereas if  $\hat{a}$  points in the direction of gravity,  $J(u)$  represents lift.

For general surfaces  $B$ , the straightforward approximation of  $J(u, p)$  by  $J(w, q)$  is not so clear because (see, for example, [18]) while  $w(\delta) \rightarrow u$  as  $\delta \rightarrow 0$ ,  $q(\delta) \rightarrow p + 1/3$  trace  $(R)$ , where  $R$  is the large eddy subgrid stress tensor

$$R_{ij} := \overline{u_i u_j} - \overline{u_i} \overline{u_j}.$$

Thus, for a general surface  $B$ ,  $q(\delta)$  is not a direct approximation to  $p$  and its use in (3.4) could skew the estimate of the force on that surface  $B$ . For a wall  $B$ , the situation is clearer. Indeed, let  $k(v) := 1/2|v|^2(x, t)$  denote the kinetic energy distribution of a velocity field  $v$ . Then we have

$$(3.5) \quad q(\delta) = p + (2/3)(k(\bar{u}) - \overline{k(u)}).$$

Since  $w$  approximates  $\bar{u}$ , the excess pressure contribution to  $q$  from  $k(\bar{u})$  is computable and thus correctable by using  $k(w)$ , but that contributed by  $\overline{k(u)}$  is not easily calculable for general surfaces. If  $B$  is a solid wall and the averaging operator, such as (2.5) and (2.6), preserves the no-slip condition, then  $k(\bar{u}) = \overline{k(u)} = 0$  on  $B$ , and  $p$  can be estimated on  $B$  by  $q(\delta)$ .

Since the boundary-force functional  $J(w, q)$ , given by (3.4), is a linear functional  $J' = J$ , we obtain the corrected approximation to the force on  $B$ :

$$(3.6) \quad \begin{aligned} J(u, p) &\sim J(w, q) - \delta J(w_\delta, q_\delta) = J(w - \delta w_\delta, q - \delta q_\delta) = \\ &\oint_B \hat{n} \cdot [(q - \delta q_\delta)I - 2\nu \nabla^s(w - \delta w_\delta)] \cdot \hat{a} \, ds. \end{aligned}$$

**3.2. Example: Flow Matching.** In flow matching, a desired velocity field  $u^*$  is specified, the flow is simulated, a functional such as

$$J(u) := \frac{1}{2} \int_{\Omega \times (0, T)} |u - u^*|^2 dx \, dt$$

is calculated, and the design or control parameters are used to drive  $J(\cdot)$  to its minimum value. Thus, one aspect of flow matching involves getting the best estimate of  $J(\cdot)$ ; this is challenging in the case of a turbulence flow.

Abstractly, given the LES velocity  $w$  and its sensitivity  $w_\delta$ , (3.2) provides an estimate of  $J(u)$  improving the estimate given by  $J(w)$ . Since  $J(\cdot)$  is quadratic, it is straightforward to calculate

$$J'(w)w_\delta = \int_{\Omega \times (0, T)} (w - w^*) \cdot w_\delta dx \, dt,$$

giving the approximation

$$(3.7) \quad J(u) \doteq \int_{\Omega \times (0, T)} \frac{1}{2} |w - u^*|^2 - \delta (w - u^*) \cdot w_\delta dx \, dt.$$

**4. Approximating Sensitivities Requires a Finer Mesh.** If the selected LES model is accurate, its solution will not vary over scales smaller than  $O(\delta)$ <sup>2</sup>. On the other hand, if the sensitivity  $w_\delta$  captures some information in fluctuations through the following expansion,

$$u \doteq w - \delta w_\delta + O(\delta^2),$$

then  $w_\delta$  will vary on scales smaller than  $O(\delta)$ . Formal asymptotics can give some preliminary insight into the width of transition regions of  $w_\delta$  (and thus into mesh

---

<sup>2</sup>A general proof of this is open for almost all LES models. Even for homogeneous isotropic turbulence, estimates are not available for the smallest persistent scale in the solution of many LES models.

design for the sensitivity equation). The correct beginning point for this is an under-resolved laminar flow with a simple, Prandtl boundary layer along a flat plate. The simplest interesting eddy viscosity is a constant  $\nu_T = O(\delta^2)$  chosen so that the  $O(\nu_T^{\frac{1}{2}})$  boundary layer in  $w$  is spread over an  $O(\delta)$  transition region. We thus suppose that  $\nu \ll \nu_T = O(\delta^2)$ , and the flow domain in the upper half plane and the model velocity approach a fixed value  $(v, 0)$ . Here  $v$  increases from  $v = 0$  to  $v = O(1)$  rapidly as  $y$  increases above the plate.

Consider thus the equilibrium problems for  $w$ ,

$$w \cdot \nabla w - (\nu + \nu_T)\delta w + \nabla q = 0,$$

and its sensitivity equation for  $s = w_\delta$ ,

$$s \cdot \nabla w + w \cdot \nabla s - (\nu + \nu_T)\delta s - \nu'_T(\delta)\delta w + \nabla q_\delta = 0.$$

We expect the x-sensitivity  $s_1$  to go from 0 to  $O(1)$  back to near 0 as  $y$  increases from the wall. Supposing that this result occurs over an  $O(\alpha)$  transition region (and following the analysis of laminar boundary layers, e.g., [8]), we consider the x-component of the sensitivity equation:

$$w_1 s_{1,x} + w_2 s_{1,y} + s_1 w_{1,x} + s_2 w_{1,y} - \nu_T(s_{1,xx} + s_{1,yy}) - \nu'_T(\delta)(w_{1,xx} + w_{1,yy}) + q_{\delta,x} = 0.$$

The relative orders of magnitude in the transition region of each term in the above equation are

$$O(1)O(1) + O(\delta)O(\alpha^{-1}) + O(1)O(1) + O(\alpha)O(\delta^{-1}) + O(\delta^2)(O(1) + O(\alpha^{-2})) + O(\delta)(O(1) + O(\delta^{-2})) = 0.$$

If we keep in mind the expectation that  $\alpha < \delta$ , the dominant terms are then  $(\frac{\delta}{\alpha})^2$  and  $\frac{1}{\delta}$ . Equating this suggests that  $\alpha \sim \delta^{\frac{3}{2}} \cong \delta^{\frac{1}{2}} \nu_T^{\frac{1}{2}}$ , suggesting that *the sensitivity equation has a boundary layer in this case thinner than that of  $w$  by a factor of  $\delta^{\frac{1}{2}}$* . This prediction is confirmed in the numerical tests in Section 5; see especially Figure 5.5.

**5. Numerical Simulations.** We use the FreeFem package [11] to validate the analytical findings concerning the width of the boundary layer of the sensitivity  $w_\delta$  and to assess the estimation potential of the sensitivity-based method.

For validation, we used a fine mesh to calculate the “truth” Navier-Stokes solution corresponding to  $\delta = 0$ . The “truth” sensitivities of the model are calculated on that fine mesh by divided differences as outlined in Section 2. In this way we uncouple the important issue of continuous vs. discrete sensitivities from evaluating either’s potential for improved estimation of flow functionals. The “truth” mesh is displayed in Figure 5.1. Of course, normally the LES+sensitivity calculations are performed on a mesh coarser than required for the Navier-Stokes equation, and numerical errors in the sensitivity calculation must be studied. For first steps in the numerical analysis of sensitivity equations in computational fluid dynamics, see [17].

**5.1. Computational Setup.** For our numerical simulations, we consider the rectangular domain from Figures 5.2 and 5.3. The domain is 8 units long and 2 units wide. A disk of radius 0.15 is placed at (3, 1). We impose no-slip boundary conditions on the horizontal walls and on the boundary of the disk, a do-nothing condition at

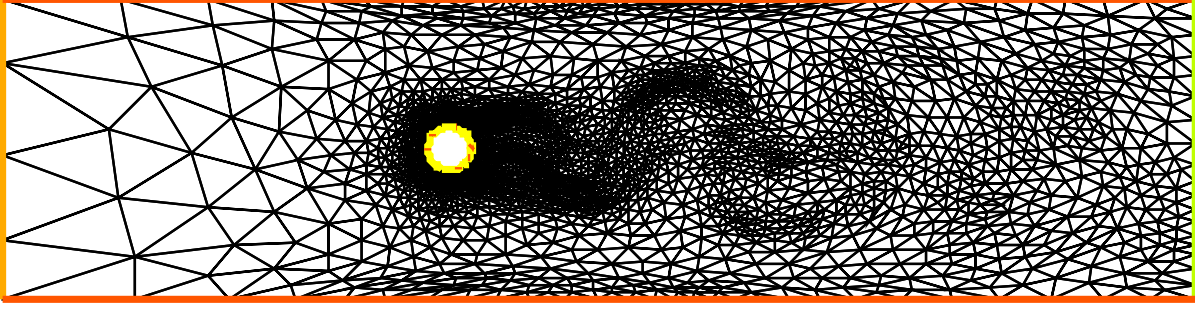


FIG. 5.1. *Final mesh.*

the outflow (right) boundary, and a time-independent parabolic profile at the inflow boundary, with the rule  $3y(2 - y)$ . As initial conditions we use the solution of the steady-state Stokes problem with the same boundary conditions.

We use an implicit-explicit time-stepping scheme to approximate the solution of the equation (2.1) :

$$(5.1) \quad \frac{w^{k+1} - w^k}{\Delta t} + \nabla \cdot (w^k w^k) - \nu \Delta w^{k+1} + \nabla q^{k+1} - \nabla \cdot (\nu_T(\delta, w^k) \nabla^s w^{k+1}) = 0, \\ \nabla \cdot w^{k+1} = 0,$$

where we denote the velocity at time step  $k$  by  $w^k$ . The problem is subsequently discretized in space by a Taylor-Hood finite element from FreeFem [11], and is implemented as a FreeFem script, where, given  $w^k$ , we compute  $w^{k+1}$ . We choose a time step  $\Delta t = 0.015$  and an inverse of the Reynolds number  $\nu = \frac{1}{200}$ , and we run the computation for 500 steps. The mesh is initialized to have around 10,000 degrees of freedom on the first pass and is subsequently refined every 50 time steps. The final mesh is presented in Figure 5.1. We use the Smagorinsky model (2.2) with an appropriate choice of  $\delta$ , specified below.

In Figures 5.2 and 5.3, respectively, we have presented the contour plot of the Euclidean norm of the velocity and the square root of the absolute value of the vorticity at four time steps of the simulation for  $\delta = 0$ . In the latter case, we chose the square root of the vorticity as a function to plot because it has the same contour plot as the vorticity function but is more sensitive in the range of interest. The results show a time-periodic behavior where vortices are generated behind the disk and shed by the flow; which is what was observed in other computational studies. Animations of the simulations that more clearly support this observation can be found at the website [1]. The result of the Navier-Stokes simulation at 7.5 seconds, which thus represents a realistic velocity distribution, is the starting point for our sensitivity estimations.

**5.2. Evaluation the Boundary Layer of the Sensitivity.** We computed the sensitivity at time 7.5 seconds by running the numerical scheme (5.1) for one time step with  $\delta = 0.05$ , denoting the result by  $\hat{w}^k$ , and one time step with  $\delta = 0$ , denoting the result by  $w^k$  and approximating the sensitivity as

$$w_\delta^k = \frac{\hat{w}^k - w^k}{\delta}.$$



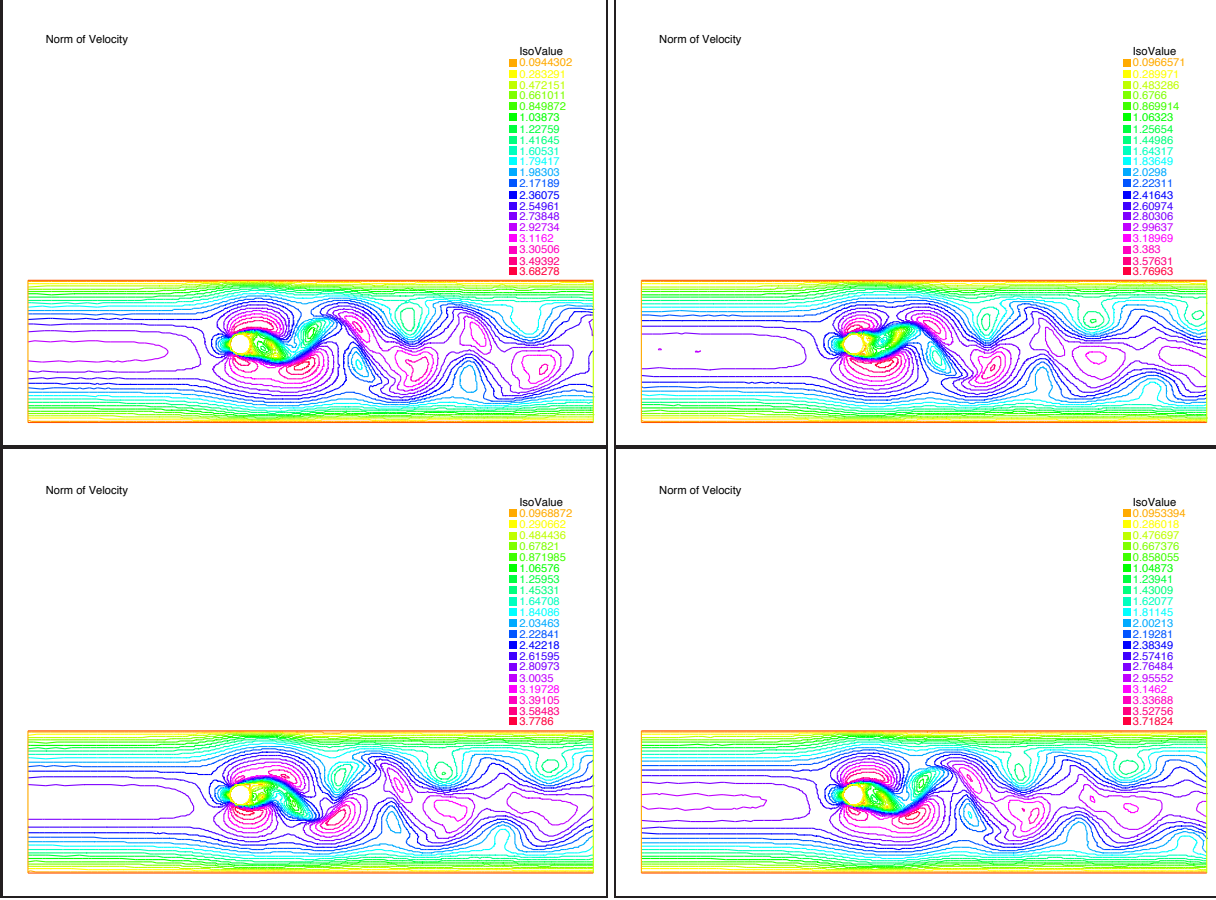


FIG. 5.2. Contour plot of the velocity at 1.65 second time intervals, ending with the snapshot at 7.5 seconds.

In Figure 5.4 we plot side by side  $w^k$  and  $|w^k - \hat{w}^k|$  (sensitivity scaled by  $\delta$ ), where the latter is measured in the local 2-norm. The results show that the largest sensitivity occurs roughly at  $\pm \frac{3\pi}{4}$ , which is also the place where the boundary layer appears to be the thinnest for the velocity  $w^k$ .

Subsequently, we computed the  $w^k$  and  $w_\delta^k$  profile on a direction that originates on the center of the disk at the angle  $-0.79\pi$ . In Figure 5.5 we plot the scaled versions of the sensitivity  $|w_\delta^k|$ , the velocity  $|w^k|$ , and the sensitivity  $|w_\delta^k|$  stretched by  $\delta^{-0.5}$ , which we denote by  $|w_\delta^k(\delta^{-0.5})|$ . The scaling is done by dividing the data to the largest values of the respective quantities along the specified direction. We see that the position of the maximum of the stretched sensitivity  $|w_\delta^k(\delta^{-0.5})|$  coincides with the maximum of the velocity  $|w^k|$ , which validates our theoretical finding that the boundary layer of the sensitivity is  $\delta^{0.5}$  thinner than the boundary layer of the velocity.

**5.3. Functional Estimation.** We now turn to the problem of estimating functionals of the Navier-Stokes flow  $\delta = 0$  using computations with  $\delta \neq 0$  followed by sensitivity-based correction. In our computations, we consider the computation of the drag functional (3.4) using the correction (3.6).

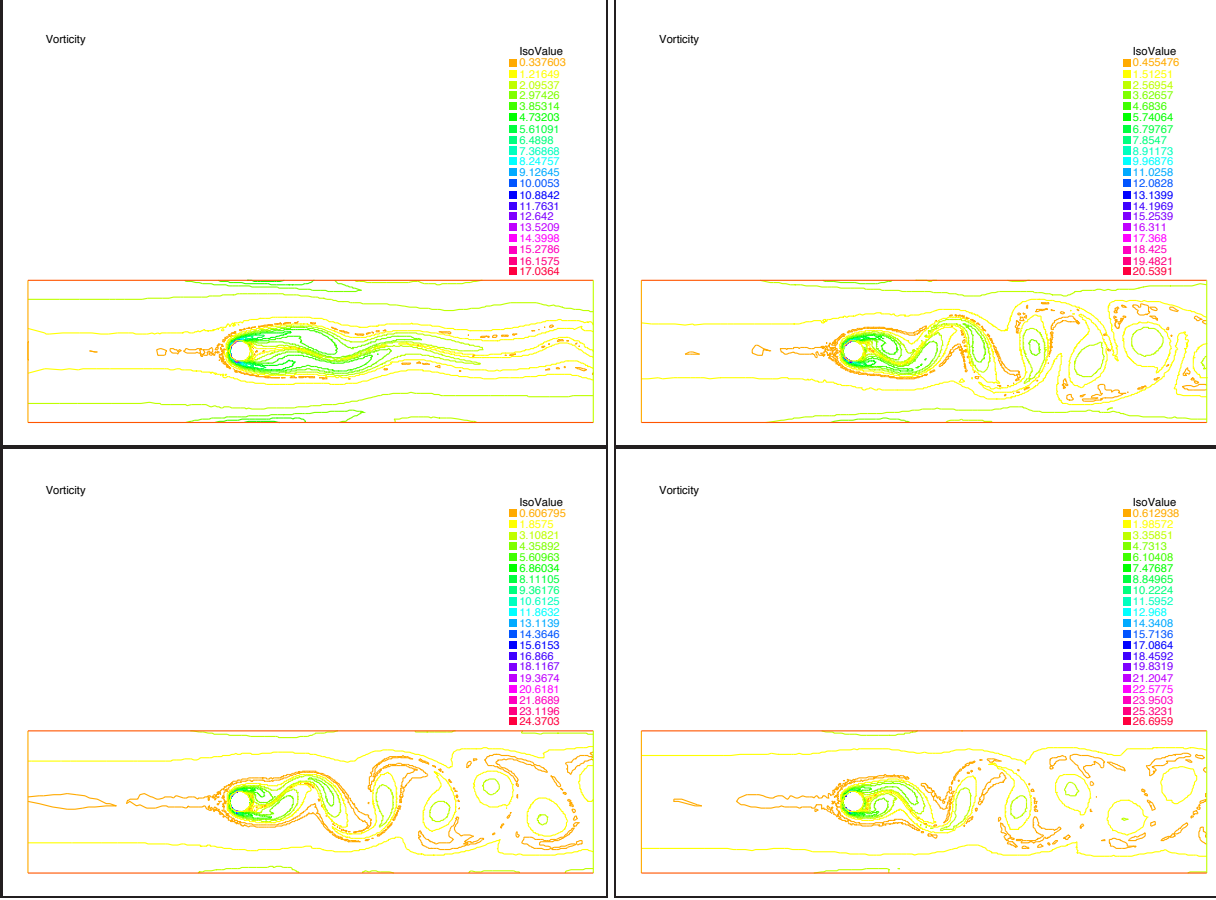


FIG. 5.3. Contour plot of the square root of the vorticity at 1.65 seconds time intervals, ending with the snapshot at 7.5 seconds.

Since we use a mesh that is finer than the one needed to resolve the sensitivity  $w_\delta$ , and since the correction of the functional (3.4) is a linear function of  $w_\delta$ , determining  $w_\delta$  by divided differences and then using it in the correction is equivalent to computing the drag functional for  $\delta \neq 0$  and then using divided differences for drag estimation at 0.

We computed the drag functional on the disk in the  $x$  direction, from the pressure and velocity derivative data, obtained from running the Smagorinsky model for one 0.015 second time step for the  $\delta$  in Table 5.1. The computed values are presented in Table 5.1, with entry “Direct Computation” in the “Method” column. We see that the correction using first-order sensitivities (linear correction) (3.6) results in a 57% reduction of the relative error, whereas correction using second-order sensitivities (quadratic correction) results in a 93% reduction of the relative error, both compared to the case where the drag is estimated by using only its value at  $\delta = 0.2$ . We represent these results graphically in Figure 5.6. Both the corrected values and their methods are listed in Table 5.1.

While we did not explicitly describe a higher-order sensitivity development, that extension is straightforward, and we interpret the above results as evidence of the

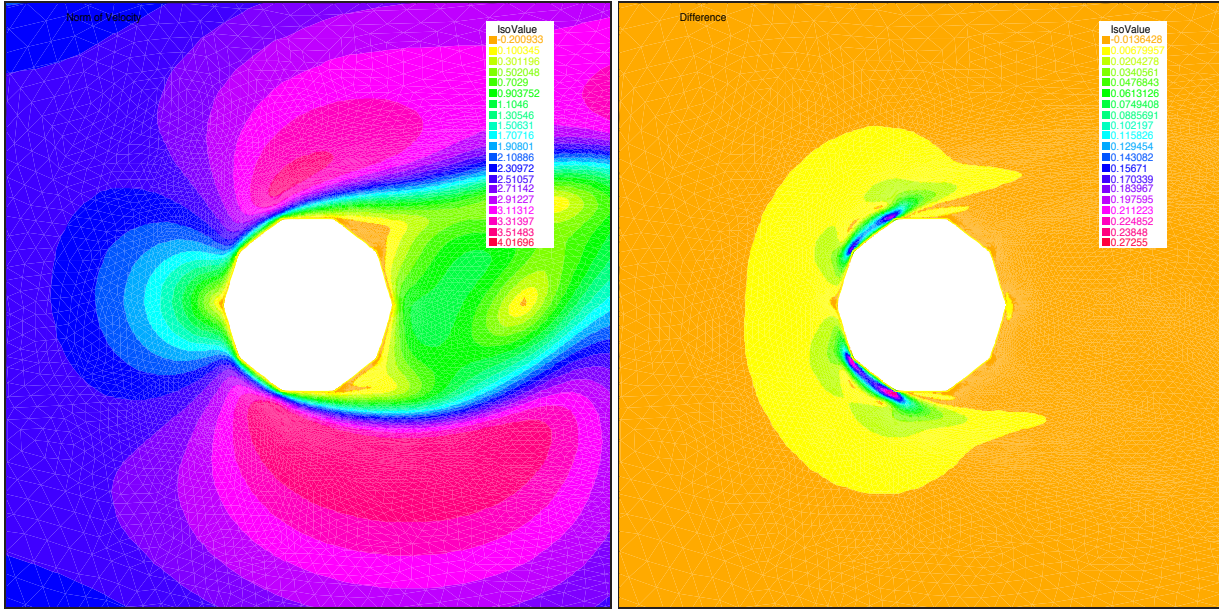


FIG. 5.4. Velocity and sensitivity at 7.5 seconds.

$\delta$	Drag	Method
0.25	-17.20	Direct Computation
0.225	-17.96	Direct Computation
0.2	-18.86	Direct Computation
0.0	-31.59	Direct Computation
0.0	-26.08	Linear Correction
0.0	-30.65	Quadratic Correction

TABLE 5.1  
Drag values

excellent potential of the sensitivity-based estimation method, described in this work.

**6. Conclusions and Future Prospects.** Many fundamental theoretical questions in LES are still open, and many of these are important for the validation of the sensitivity approach to estimating model uncertainty. Nevertheless, we have seen that the continuous sensitivity equation approach in these tests has given a remarkably accurate estimate of the solution change as the lengthscale parameter varies *provided the sensitivity equation is appropriately resolved* itself. Formal asymptotics gives estimates of the mesh-resolution requirements of the continuous sensitivity equation that are, again, remarkably accurate in our test.

The success of the sensitivity equation approach as shown here (and in other tests) suggests its broader usefulness and hints at the possibility of establishing a general, analytic foundation for the method in LES.

**Acknowledgments.** We are grateful to Paul Fischer for helpful comments that have improved the quality of the paper. Mihai Anitescu was supported by the Mathematical, Information, and Computational Sciences Division subprogram of the Office of Advanced Scientific Computing Research, Office of Science, U.S. Department of En-

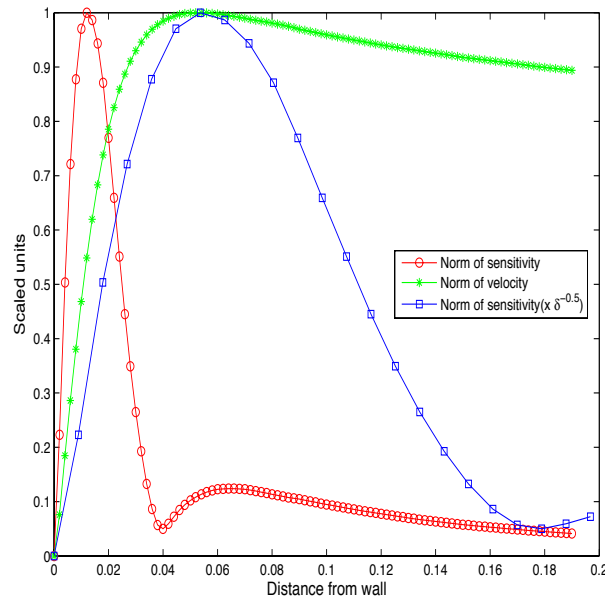


FIG. 5.5. Comparison of the scaled sensitivity and velocity on a direction at  $-0.79\pi$  from the center of the disk.

ergy, under Contract W-31-109-ENG-38. William J. Layton was partially supported by NSF grants DMS 9972622, INT 9814115 and DMS 0207627.

#### REFERENCES

- [1] M. ANITESCU. url=<http://www.mcs.anl.gov/~anitescu/FLUIDS/fluids.htm>.
- [2] L. C. BERSELLI, T. ILIESCU, AND W. J. LAYTON, *Mathematics of Large Eddy Simulation of Turbulent Flows*, Springer-Verlag, Berlin, (expected) 2005.
- [3] J. BORGGAARD AND J. BURNS, *A PDE sensitivity equation method for optimal aerodynamic design*, Journal of Computational Physics, 136 (1997), pp. 366–384.
- [4] J. BORGGAARD AND A. VERMA, *Solutions to continuous sensitivity equations using automatic differentiation*, SIAM Journal of Scientific Computing, 22 (2001), pp. 39–62.
- [5] Q. DU AND M. GUNZBURGER, *Analysis of a Ladyzhenskaya model for incompressible viscous flow*, Journal of Mathematical Analysis and Applications, 155 (1991), pp. 21–45.
- [6] A. DUNCA, V. JOHN, AND W. LAYTON, *The commutation error of the space averaged Navier Stokes equations on a bounded domain*, in Contributions to Current Challenges in Mathematical Fluid Mechanics, Advances in Mathematical Fluid Mechanics 3, G. Galdi, J. Heywood, and R. Rannacher, eds., Birkhauser Verlag Basel, 2004, pp. 53–78.
- [7] M. GERMANO, *Differential filters for the large eddy simulation of turbulent flows*, Physics of Fluids, 29 (1986), pp. 1755–1757.
- [8] S. GOLDSTEIN, *Modern Developments in Fluid Dynamics*, vol. 1, Dover, New York, 1965.
- [9] M. GUNZBURGER, *Sensitivites, adjoints, and flow optimization*, Inter. J. Num. Meth. Fluids, 31 (1999), pp. 53–78.
- [10] ———, *Practical and Theoretical Perspectives in Flow Control and Optimization*, SIAM, Philadelphia, 2002.
- [11] F. HECHT, O. PIRONNEAU, AND K. OHTSUKA, *Freefem++ manual*. url=<http://www.freefem.org>.
- [12] T. ILIESCU AND W. LAYTON, *Approximating the larger eddies in fluid motion III: The Boussinesq model for turbulent fluctuations*, Analele Stiintifice ale Universitatii “Al. I. Cuza” Iasi, 44 (1998), pp. 245–261.
- [13] V. JOHN, *Large Eddy Simulation of Turbulent Incompressible Flows. Analytical and Numerical Results for a Class of LES Models*, vol. 34 of Lecture Notes in Computational Science and Engineering, Springer-Verlag, Berlin, 2004.

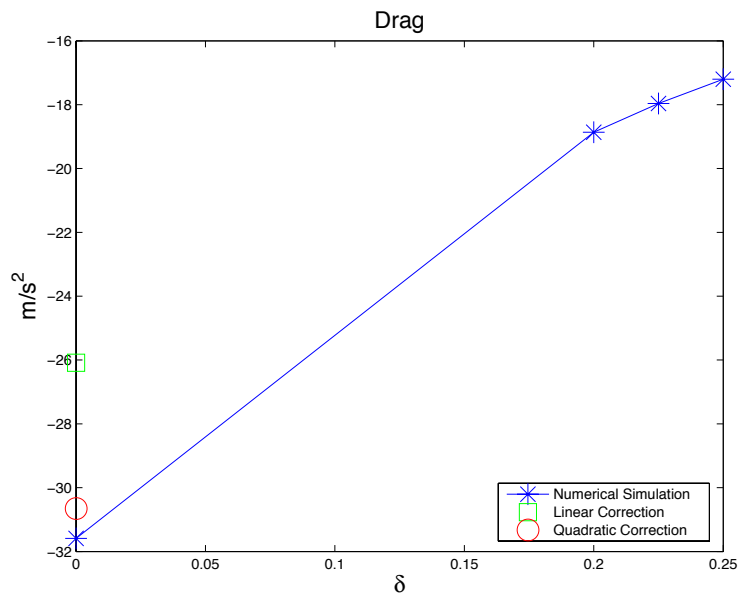


FIG. 5.6. Computed drag as a function of  $\delta$  and corrected drag

- [14] V. JOHN, W. LAYTON, AND N. SAHIN, *Derivation and analysis of near wall models for channel and recirculating flows*, Computers and Mathematics with Applications, 48 (2004), pp. 1135–1151.
- [15] M. KAYA AND W. LAYTON, *On verifiability of models of the motion of large eddies in turbulent flows*, Differential and Integral Equations, 15 (2002), pp. 1395–1407.
- [16] W. LAYTON AND R. LEWANDOWSKI, *Analysis of an eddy viscosity model for large eddy simulation of turbulent flows*, Journal of Mathematical Fluid Mechanics, 2 (2002), pp. 374–399.
- [17] F. PAHLEVANI, *Sensitivity analysis of eddy viscosity models*, PhD thesis, Department of Mathematics, University of Pittsburgh, 2004.
- [18] P. SAGAUT, *Large Eddy Simulation for Incompressible Flows*, Springer, New York City, 2001.
- [19] P. SAGAUT AND T. LE, *Some investigations of the sensitivity of large eddy simulation*, Tech. Rep. 1997-12, ONERA, Toulouse, France, 1997.
- [20] L. STANLEY AND D. STEWART, *Design sensitivity analysis: Computational issues of sensitivity equation methods*, in Frontiers in Mathematics, SIAM, Philadelphia, 2002.

The submitted manuscript has been created by the University of Chicago as Operator of Argonne National Laboratory (“Argonne”) under Contract No. W-31-109-ENG-38 with the U.S. Department of Energy. The U.S. Government retains for itself, and others acting on its behalf, a paid-up, nonexclusive, irrevocable worldwide license in said article to reproduce, prepare derivative works, distribute copies to the public, and perform publicly and display publicly, by or on behalf of the Government.